Inpainting techniques for metal artifact reduction in Computed Tomography images

E. Faggiano

[1] MOX - Department of Mathematics - Politecnico di Milano

[2] LabS - Department of Chemistry, Material and Chemical Engineering - Politecnico di Milano

June 7, 2014

X Ray

La tecnica diagnostica si basa sull'assorbimento da parte della materia dei raggi incidenti.

Raggi X = fotoni con lunghezza d'onda λ caratterizzati da una energia

$$E = \nu h = \frac{hc}{\lambda}$$

dove c ÃÍ la velocitÃă della luce, h la costante di Plank e ν la frequenza dell'onda.

1. Energie coinvolte sono dell'ordine di 12-124 KeV (contro gli 1.8-3.1 KeV della luce) : lunghezze d'onda molto piccole e frequenze molto elevate.
2. Funzionamento: misuro l'attenuazione subita dal fascio entrante nel corpo.

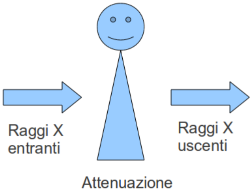

X Ray

$$N = N_0 \exp(-\mu x) \tag{1}$$

Attenuazione dei raggi = assorbimento per effetto fotoelettrico + diffusione per effetto Compton

- N_0 = numero fotoni incidenti
- N = numero fotoni emergenti
- μ = attenuazione lineare che dipende da numero atomico e densitÃă

Muscolo e grasso hanno bassa attenuazione. L'osso ha alta attenuazione.

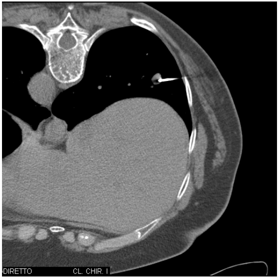

Dispositivi per rilevazione raggi X

Dispositivo ÃÍ caratterizzato da un generatore di raggi X e da un rilevatore:
1. Pellicola radiografica: classica radiografia, immagine proiettiva.

Dispositivi per rilevazione raggi X

2. Tomografia Computerizzata (CT o TAC):
   - i rilevatori possono essere solidi o a gas e hanno risposta lineare all'energia dei raggi X
   - le ultime generazioni sono di tipo elicoidale per l'acquisizione con un solo passaggio dei dati dell'intero volume. Le ultime generazioni sono anche multistrato.L'avanzamento del lettino puÃš essere pari, inferiore o maggiore allo spessore delle fette.

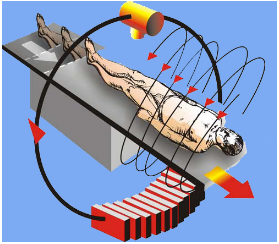

   - dal dato grezzo collezionato dai rilevatori all'immagine fruibile si passa tramite algoritmi di ricostruzione da proiezioni (fitered back projection).

Dispositivi per rilevazione raggi X

- il dato finale ÃÍ composto da matrici di voxel (risoluzioni possono variare 0.1 mm a 6 mm).
- ogni voxel ha un valore pari al valore di attenuazione del materiale in quella regione volumetrica misurata in unitÃă Hounsfield

$$\mu(HU) = \frac{\mu - \mu_{H_2O}}{\mu_{H_2O}} 1000 \tag{2}$$

  tessuti molli = attenuazione simile all'acqua = 0
  osso compatto = attenuazione alta circa 1000
  aria = attenuazione praticamente nulla circa -1000
  I valori sono rappresentati in scala di grigio.
- si possono acquisire immagini in diversi istanti del ciclo caridaco tramite dispositivi di triggering che sincronizzano l'acquisizione col segnale ECG e/o col segnale respiratorio.

3. altri (cineradiografia, radiografia computerizzata...)

X-ray computed tomography (CT) images

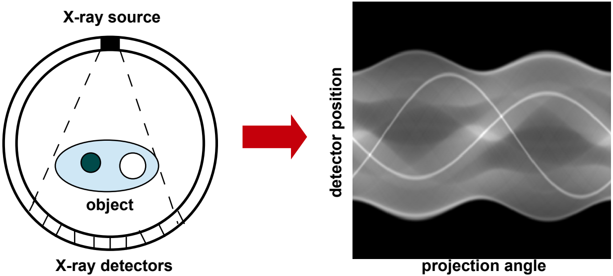

- Signal collected by the array of detectors is the X-ray attenuation.
- Signal attenuation is proportional to material density and to the pass lenght.
- Signal collected by CT detectors is organized, in function of projection angle and detector position, in the so-called sinogram matrix.

Metal Artifact in X-ray computed tomography (CT)

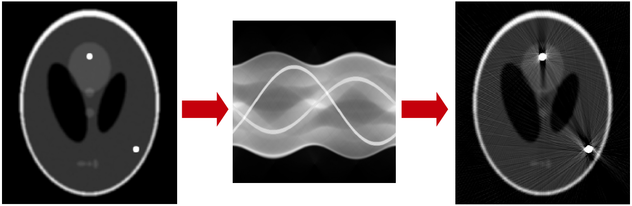

- Commonly observed in images of patients with permanent metallic implants (*e.g.* dental fillings, hip prostheses, cardiac devices etc.).
- The high X-ray attenuation of the metallic parts allows only a limited number of photons to reach the CT detectors.
- Combination of phenomenon known as beam hardening and scattering.
- In synthesis metal artifacts lead to inconsistent sinogram projections, which alter the image reconstruction process.

Metal Artifact Reduction (MAR) techniques

Various approaches have been proposed:

- iterative reconstruction methods
- interpolation-based methods

Metal Artifact Reduction (MAR) techniques

Various approaches have been proposed:

- iterative reconstruction methods:
  - modified versions of classical iterative reconstruction algorithms
  - original raw projection data from the scanner is stored in a proprietary format, and therefore not always accessible
  - high computational costs

  - two main groups: algebraic techniques (*e.g.* algebraic reconstruction and simultaneous iterative reconstruction [Wang et al., 1996, Robertson et al., 1997]) and statistical techniques (*e.g.* maximum likelihood-expectation maximization algorithms [De Man et al., 1999, Nuyts et al., 1999])

Metal Artifact Reduction (MAR) techniques

Various approaches have been proposed:

- interpolation-based methods:
  - identification of the corrupted parts of the sinogram and replacement using information coming from the uncorrupted neighboring projections
  - less computationally expensive
  - do not require original raw projection data

  - strategies include, among others, linear interpolation (LI) [Kalender et al., 1987], cubic interpolation [Bazalova et al., 2007], spline interpolation [Abdoli et al., 2009], wavelet based interpolation [Zhao et al., 2000] and techniques involving partial differential equation (PDE) [Duan et al., 2008, Zhang et al., 2011].

Metal Artifact Reduction (MAR) techniques - interpolation-based

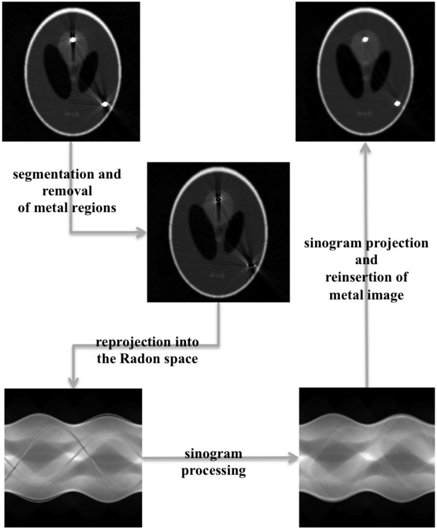

- Sinogram processing through image inpainting !

Image inpainting

- restoration of old/damaged photos;
- the idea is that the missing parts (damaged parts) of an image can be filled using information diffused from the nearby areas through a suitable PDE.

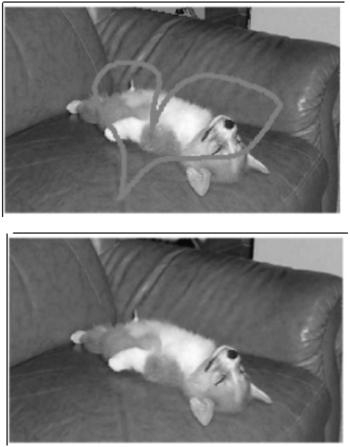

from [Bertozzi et al., 2007b]

Image inpainting

Main methods:

- Fourier's Heat Equation (HE): simplest way. Disadvantage: due to its regularization property, this equation cannot preserve discontinuous image features.
- Total Variation (TV) flow [Shen and Chan, 2002]: the diffusivity constant depends upon the size of the image gradient, so that diffusion near edges is namely reduced. Disadvantage: does not perform well on edges spanning large gaps.
- Euler's Elastica (EE) [Shen et al., 2003]: allows for connection across large distances.
- Chan-Hilliard (CH) equation and TV-H^{-1} method [Bertozzi et al., 2007b, Burger et al., 2009]: same good properties as the EE method and, in addition, can be solved by fast computational techniques [Bertozzi et al., 2007a].
- Naver-Stokes equations [Bertalmio, et. al, 2001].

Inpainting

- A 2D image can be identified with a domain $\Omega \subset \mathbb{R}^2$ (i.e. the image domain) and a function I^0 standing for the image intensity distribution over Ω.
- The area of the image to be inpainted can be considered as a set $D \subset \Omega$ (i.e. the inpainting domain) and the inpainting problem consists in using the values attained by the I^0 function in $\Omega \setminus D$ to find a distribution $\widetilde{I}$ that fills properly D.

Navier Stokes inpainting

- Idea: transport the gradient of the smoothness of the image intensity in the direction of the contour lines (or the isophotes)
- We know that the contour lines can be represented as $\nabla^{\perp} I$.
- The smoothness of the image which contains information about the borders of objects is ΔI.

$\Longrightarrow$ the method translates in solving :

$$I_t = \nabla^{\perp} I \cdot \nabla \Delta I$$

in the inpainting domain D. This is a transport equation that convects the image intensity I along level curves of the smoothness ΔI.
The goal is to evolve the previous equation to a steady state which becomes:

$$\nabla^{\perp} I \cdot \nabla \Delta I = 0$$

Navier Stokes inpainting

Analogy to transport of vorticity in incompressible fluids

Navier-Stokes equations for incompressible Newtonian fluids:

$$\begin{cases} v_t + v \cdot \nabla v - \nu \Delta v + \nabla p = 0 \\ \nabla \cdot v = 0 \end{cases}$$

in two space dimension the divergence free velocity field v possesses a stream function Ψ satisfying $v = \nabla^\perp \Psi$. If we take the curl of the first equation, we obtain an equation in the vorticity ω:

$$\begin{cases} \omega_t + v \cdot \nabla \omega - \nu \Delta \omega = 0 \\ \omega = \mathrm{rot}(v) = \mathrm{rot}(\nabla^\perp \Psi) = \Delta \Psi \end{cases}$$

In terms of stream function, steady state must satisfy:

$$v \cdot \nabla \omega - \nu \Delta \omega = \nabla^\perp \Psi \cdot \nabla \Delta \Psi - \nu \Delta \Delta \Psi \ = 0$$

which, for inviscid fluids, becomes

$$\nabla^\perp \Psi \cdot \nabla \Delta \Psi = 0$$

which says that the Laplacian of the stream function, and hence the vorticity, must have the same level curves as the stream function.

Navier Stokes inpainting

Analogy to transport of vorticity in incompressible fluids

Navier-Stokes	Image inpainting
stream function Ψ	Image intensity I
fluid velocity $v = \nabla^\perp \Psi$	isophote direction $\nabla^\perp I$
vorticity $\omega = \Delta \Psi$	smoothness $\omega = \Delta I$
fluid viscosity ν	anisotropic diffusion ν

We solve:

$$\begin{cases} v \cdot \nabla v - \nu \Delta v + \nabla p = 0 \\ \nabla \cdot v = 0 \end{cases}$$

and

$$\Delta I = \mathrm{rot}(v)$$

with $\nu(\|\nabla^\perp I\|) = \frac{1}{1+\frac{\|\nabla^\perp I\|}{k}}$ (k tuning parameter).
less viscous where velocity is high (to avoid too much diffusion).

Navier Stokes inpainting

B.C: Ω is the inpainting domain and I_{orig} the intensity distribution of the sinogram image.
We impose:

$$\begin{cases} v(\cdot,0) = v(\cdot,2\pi) \\ v = \nabla^{\perp} I_{orig} \qquad \delta\Omega \setminus \{(r,\theta) | \theta = 0 \vee \theta = 2\pi\} \end{cases}$$

while in the problem $\Delta I = \mathrm{rot}(v)$ we impose:

$$\begin{cases} I(\cdot,0) = I(\cdot,2\pi) \\ I = I_{orig} \qquad \delta\Omega \setminus \{(r,\theta) | \theta = 0 \vee \theta = 2\pi\} \end{cases}$$

Navier Stokes inpainting - our framework

- Solve for the velocity:
- To compute the gradient on $\delta\Omega$ we dilate Ω and we compute the gradient using a 8-node stencil;
- Finite element method with $P1_b$ - $P1_b$ (velocity) and $P1$ (pressure);
- fixed point method with initial condition the solution of the Stokes equation;
- the linear system is solved with a preconditioned GMRES (pressure mass preconditioning).
- Stopping criteria:

$$\frac{\|v_k - v_{k-1}\|_{H^1}}{\|v_0\|_{H^1}} \leq \epsilon$$

- Solve for I

Metal Artifact Reduction (MAR) techniques - interpolation-based

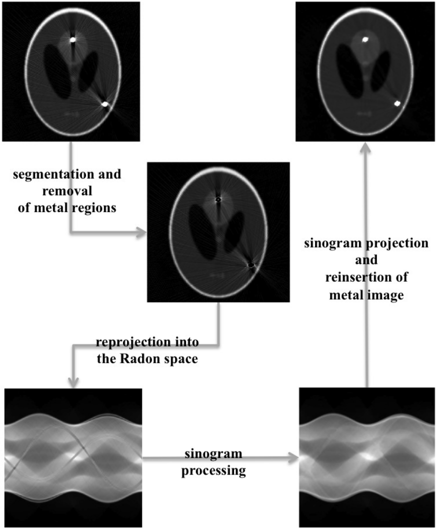

- Sinogram processing through Navier-Stokes inpainting

Results - synthetic data

A Shepp-Logan phantom of 256×256 pixels with three metal regions of high attenuation and induced artifacts is generated.

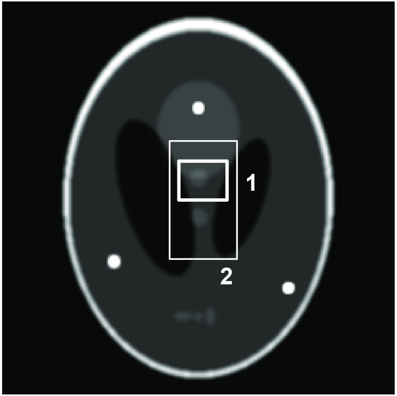

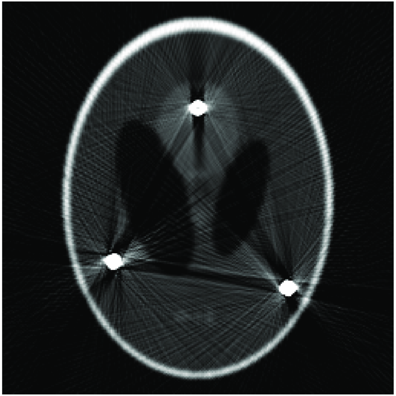

Results - synthetic data

OI

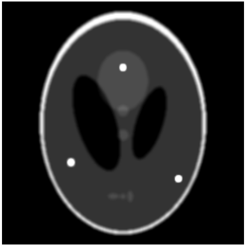

PA

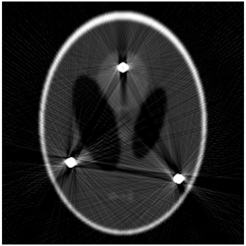

LI

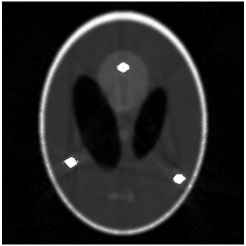

HE

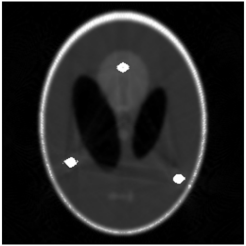

TV

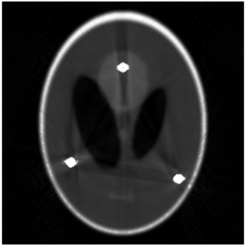

NS

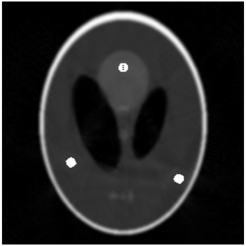

Results - synthetic data - Region 1

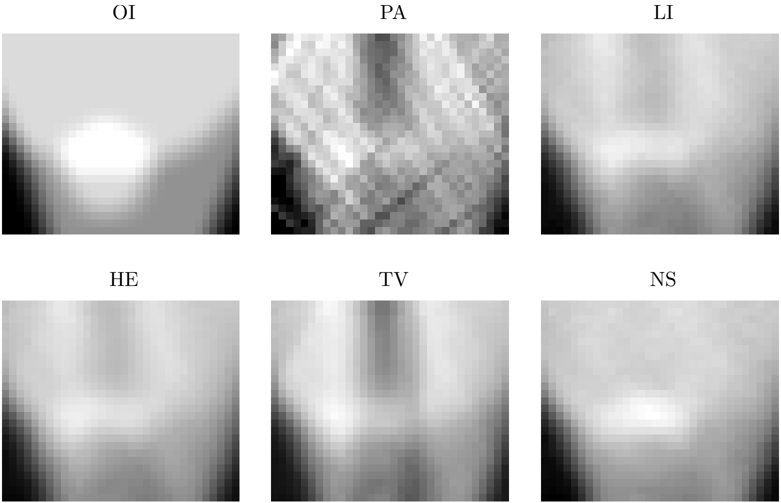

Results - one example on a clinical image

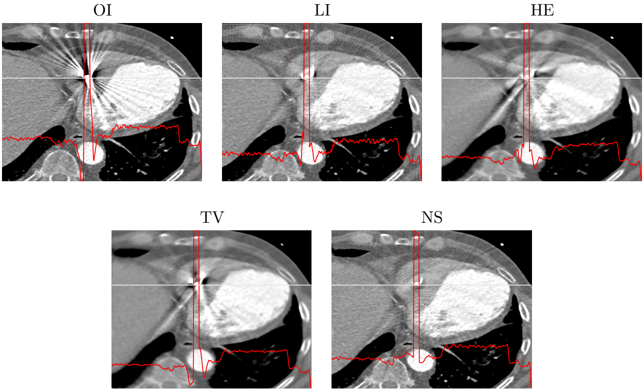

- bright fictitious artifacts are introduced by the HE and TV method.
- Profile-lines: metallic implants result into high picks, while dark-band artifacts correspond to concavities;
- frequent small changes dominate the LI profile;
- NS profile is smoother with concavities of lower attenuation much less evident;

Results - one example on a clinical image

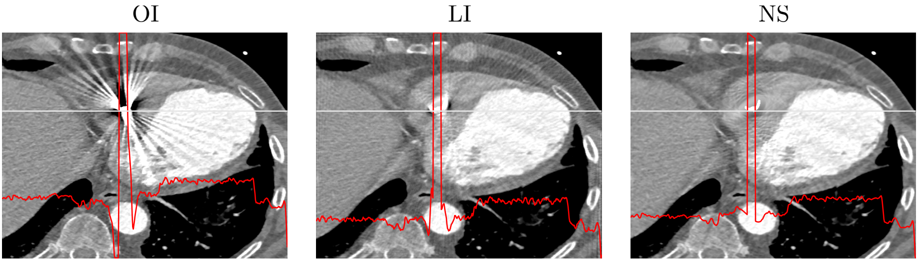

Results - one example on a clinical image

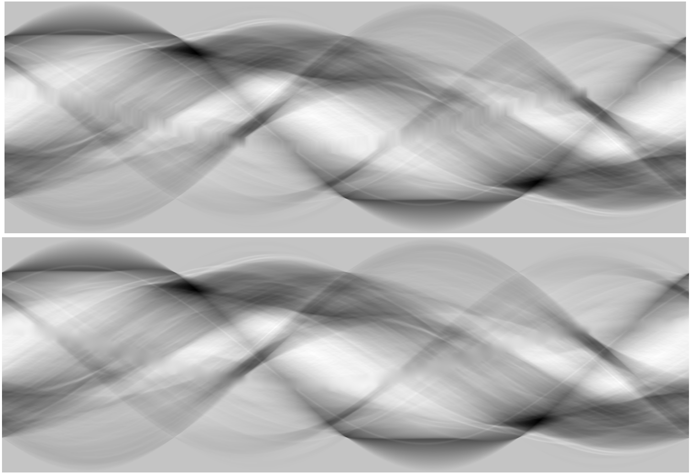

Figure: Inpainted sinogram with Linear interpolation and with NS

References I

Abdoli, M., Ay, M. R., Ahmadian, A., and Zaidi, H. (2009).
Reduction of dental filling metallic artifacts in ct-based attenuation correction of pet data using weighted virtual sinograms.
In *Nuclear Science Symposium Conference Record (NSS/MIC), 2009 IEEE*, pages 2752–2755. IEEE.

Bazalova, M., Beaulieu, L., Palefsky, S., and Verhaegen, F. (2007).
Correction of ct artifacts and its influence on monte carlo dose calculations.
Medical physics, 34:2119.

Bertozzi, A., Esedoglu, S., and Gillette, A. (2007a).
Analysis of a two-scale cahn-hilliard model for binary image inpainting.
Multiscale Modeling & Simulation, 6(3):913–936.

Bertozzi, A. L., Esedoglu, S., and Gillette, A. (2007b).
Inpainting of binary images using the cahn–hilliard equation.
Image Processing, IEEE Transactions on, 16(1):285–291.

Burger, M., He, L., and Schönlieb, C.-B. (2009).
Cahn-hilliard inpainting and a generalization for grayvalue images.
SIAM Journal on Imaging Sciences, 2(4):1129–1167.

De Man, B., Nuyts, J., Dupont, P., Marchal, G., and Suetens, P. (1999).
Reduction of metal streak artifacts in x-ray computed tomography using a transmission maximum a posteriori algorithm.
In *Nuclear Science Symposium, 1999. Conference Record. 1999 IEEE*, volume 2, pages 850–854. IEEE.

Duan, X., Zhang, L., Xiao, Y., Cheng, J., Chen, Z., and Xing, Y. (2008).
Metal artifact reduction in ct images by sinogram tv inpainting.
In *Nuclear Science Symposium Conference Record, 2008. NSS'08. IEEE*, pages 4175–4177. IEEE.

References II

Kalender, W. A., Hebel, R., and Ebersberger, J. (1987).
Reduction of ct artifacts caused by metallic implants.
Radiology, 164(2):576–577.

Nuyts, J., De Man, B., Dupont, P., Defrise, M., Suetens, P., and Mortelmans, L. (1999).
Iterative reconstruction for helical ct: a simulation study.
Physics in medicine and biology, 43(4):729.

Robertson, D. D., Yuan, J., Wang, G., and Vannier, M. W. (1997).
Total hip prosthesis metal-artifact suppression using iterative deblurring reconstruction.
Journal of computer assisted tomography, 21(2):293–298.

Shen, J. and Chan, T. F. (2002).
Mathematical models for local nontexture inpaintings.
SIAM Journal on Applied Mathematics, 62(3):1019–1043.

Shen, J., Kang, S. H., and Chan, T. F. (2003).
Euler's elastica and curvature-based inpainting.
SIAM Journal on Applied Mathematics, 63(2):564–592.

Wang, G., Snyder, D. L., O'Sullivan, J., and Vannier, M. (1996).
Iterative deblurring for ct metal artifact reduction.
Medical Imaging, IEEE Transactions on, 15(5):657–664.

Zhang, Y., Pu, Y.-F., Hu, J.-R., Liu, Y., Chen, Q.-L., and Zhou, J.-L. (2011).
Efficient ct metal artifact reduction based on fractional-order curvature diffusion.
Computational and mathematical methods in medicine, 2011.

References III

Zhao, S., Robeltson, D., Wang, G., Whiting, B., and Bae, K. T. (2000).
X-ray ct metal artifact reduction using wavelets: an application for imaging total hip prostheses.
Medical Imaging, IEEE Transactions on, 19(12):1238–1247.

Thank you

Inpainting from a variational and PDE perspective

- The general form of such a variational inpainting approach is:

$$\widetilde{u} = \min_{u \in H_1} \left\{ E(u) = \lambda || \chi_{\Omega \setminus D}(u^0 - u)||^2_{H_2} + R(u) \right\}, \tag{3}$$

- H_1 and H_2 are Banach spaces on Ω.

- The first term of the right-hand side is the so-called fidelity term, which keeps memory of the original image. $\chi_{\Omega \setminus D}$ is the characteristic function of $\Omega \setminus D$, λ is a coefficient.

- The second term is the so-called regularizing term.

- The definition of the regularizing term and Banach spaces characterizes the inpainting method.

- minimization translates in evolving to a steady state a PDE.